International Conference on Artificial Reality and Telexistence
Eurographics Symposium on Virtual Environments (2022)
J.-M. Normand and H. Uchiyama (Editors)

Characteristics of Background Color Shifts Caused by Optical See-Through Head-Mounted Displays

Daichi Hirobe[†1], Yuki Uranishi[1], Jason Orlosky[1,2], Shizuka Shirai[1], Photchara Ratsamee[3] and Haruo Takemura[1]

[1] Osaka University, Japan [2] Augusta University, United States [3] Osaka Institute of Technology, Japan

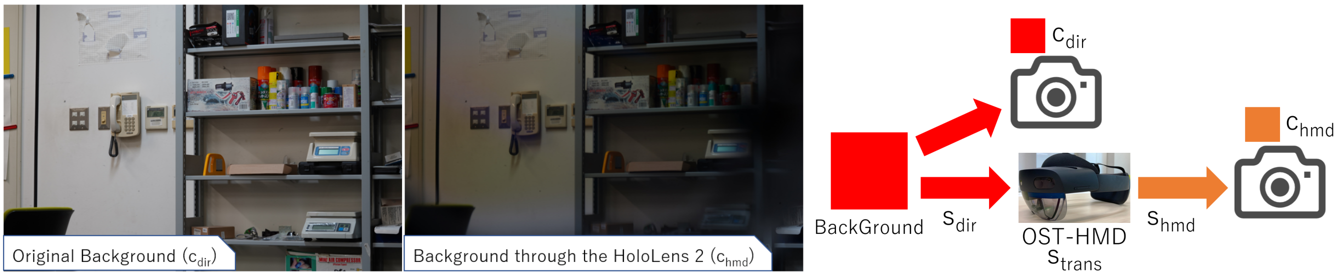

Figure 1: *Images showing how the background color seen by an OST-HMD user is shifted (left and center, taken with a SONY alpha 7 iii). We objectively measured background light directly (s_{dir}) and through an OST-HMD (s_{hmd}), and calculated the spectral transmittance of the OST-HMD (s_{trans}) (right). Light from background was measured in 429 conditions, including 3 OST-HMDs, 13 background colors, and 11 measuring areas and angles. We also evaluated these measurements by comparing c_{dir} and c_{hmd} using the CIEDE 2000 [LCR01] and discussed how shifts in background color can affect color compensation.*

Abstract

Optical see-through head-mounted displays (OST-HMDs) have been increasingly used in many applications as Augmented Reality (AR) support devices. However, problems still exist that prevent their use as general-purpose devices. One of these issues is the color blending problem. This is the problem in which light from the background overlaps with light from the OST-HMD and shifts the color of OST-HMD's light from its intended display intensity and color. Though color compensation methods exist, in order to properly compensate for light shifts, we need to know how the background color will affect the light that eventually hits the user's eye when combined with the OST-HMD image. In this paper, we study how background colors shift as a result of passing through the OST-HMD's optics in order to better inform the development of color compensation methods. We measured the background color objectively for three off-the-shelf OST-HMDs and evaluated results. We found that all three OST-HMDs shift background color to a perceptible degree and that the degree of shift depends on the original background color. We also investigated how the degree of shift differs between different areas on the OST-HMD screens and from different measuring angles. The results showed that the background color shift depends on both the area and angle measured for some OST-HMDs.

1. Introduction

Augmented Reality (AR) is expected to quickly gain adoption in a variety of fields like education [Lee12, AGBAD*21], industry [DPMS18, PYK19], and medicine [EHRSMR19, YLD*21]. Optical see-through head-mounted displays (OST-HMD) are often used for AR and overlay digital content directly onto the user's view, which makes them appropriate for supporting work that requires simultaneous viewing of both real and digital information.

However, some problems still have to be solved before these displays can be used in a wide range of situations. One of these issues is that the color of light from the display is blended with the light from the background [GSZW10, GSZ13], thereby shifting the resulting perceived color. This may cause poor content visibility and lead to incorrect operation because colors that the users perceive are different from those the developers intended. In order to address this problem, color compensation methods have been widely studied [SHRFI13, HRISI15, LCR16, ZWP*21]. Color compensation adjusts the output of the display and corrects the blended color so that it more closely matches the intended one. Precise color compensation algorithms need to know the colors of light from the display and one

[†] e-mail: hirobe.daichi@lab.ime.cmc.osaka-u.ac.jp

DOI: 10.2312/egve.20221285

from the background precisely, and in order to know the latter, it's needed to be known how the light color is shifted by passing through OST-HMDs. However, previous studies about color compensation methods treated the shift of the background color variously, and there are only a few studies about how the background color is shifted by OST-HMDs.

This study aims to investigate the shift of the background color caused by OST-HMDs. In this study, we chose three off-the-shelf OST-HMDs and objectively measured the light from the background both directly and through an OST-HMD using a spectrometer. Then, we calculated the spectral transmittance for each display, which is considered to be a major cause of the color shift, and investigated the specific characteristics of the shift itself. We divided each display into nine areas and measured for each of these areas rather than the whole display in order to discuss the uniformity of spectral transmittance among each area by comparing their measurements. We also measured the same area from different angles and investigated how spectral transmittance depends on the viewing angle.

2. Related Work

The color blending problem in OST-HMDs has been known for years, and several studies exist that explore this problem itself. In addition, methods such as color compensation algorithms have been developed to address this problem. In this section, we first describe studies about the color blending problem itself. Next, we describe various color compensation methods and how they treated the shift of the background color.

2.1. Color Blending Problem in OST-HMDs

According to the survey by Itoh et al. [ILSP21], the color blending problem in OST-HMDs was first described by Gabbard et al. [GSZW10]. They displayed the same color on an OST-HMD against six different backgrounds, black (they referred to as *no-background*), white, and four-color samples that mimic the real-world background. They examined the content colors seen by users with a colorimeter set at a position corresponding to a user's eye and found that measured colors were shifted towards the background color from the original one, which is known as "the color blending." They also made the same measurement with the real background rather than color samples and got similar results [GSZ13].

Livingston et al. [LBS] conducted a color matching experiment with 4 HMDs, including 3 OST-HMDs and 1 video see-through head-mounted display, and found that the background color affected the results. Havig et al. [HGH*01] also conducted a user experiment in which subjects were asked to identify the color and the value of digits overlaid on backgrounds that mimic the real world. They confirmed that the color blending, e.g., green digits on a brick background seemed yellow, occurred.

These studies confirmed the color blending problem in OST-HMDs objectively and subjectively. In order to address this problem, two approaches have been studied; software approaches and hardware approaches. Software approaches mainly to adjust the displayed color and make blended color desirable. On the other hand, hardware approaches mainly make the area where contents are rendered opaque and shut out the light from the background. Hardware approaches can solve the color blending problem basically, but they require special hardware and often bring other problems, e.g., narrow FoV [ILI*19], decrease in display transparency [WHL10], and low image quality [MF13]. Thus, we focused on software approaches in this study.

2.2. Color Compensation in OST-HMDs

In order to address the color blending problem, color compensation methods have been studied. Sridharan et al. [SHRFI13] proposed a method that uses a lookup table. They made a table of input sRGB values and output colors and chose an input that can show an output closest to the desired one when blended with the background. However, their method mainly focuses on correcting the OST-HMD's color distortion. So they treated the shift of the background color as out of scope and made an assumption that the background color which users perceive is known.

Hincapié-Ramos et al. [HRISI15] proposed a more practical method based on Sridharan's method. This method can search a lookup table faster by using binary search and be executed in real-time. In addition, they tried to address the shift of the background color with a linear regression of the background color that users perceive. Langlotz et al. [LCR16] also proposed a practical method that even considered hardware implementation. This method captures the background image from a half-silvered mirror and an external camera which are put in front of an OST-HMD. Then, the output color is calculated by subtracting the background from the intended output color for each pixel. Their method also uses linear regression to address the shift of the background color. However, in the paper of [HRISI15], Hincapié-Ramos et al. reported that there is an error in linear regression on $L^*a^*b^*$ color space when the original background color's L^* is low or a^*, b^* is close to 0. So they concluded that there is a room for improvement, including using other approaches than linear regression.

Zhang et al. [ZWP*21] proposed a color compensation method which not only reproduces the intended color but tries to make the contrast between the background and contents higher and improve the visibility of contents. However, they treated the shift of the background color is out of scope. Their method uses a Gaussian filtered image of an external camera as the background color which users perceive.

As we've seen, color compensation methods have been studied so far but they treated the shift of the background color variously. However, given color blending is occurred by the output light from an OST-HMD and the background light passing through an OST-HMD, knowing how the background color is shifted by an OST-HMD is essential in order to achieve precise color compensation.

2.3. Background Color Estimation

As mentioned above, precise color compensation requires precise background color estimation. Ryu et al. [RKLK16] proposed a method that estimates the background color users perceive through an OST-HMD, from an external camera image. This method consists of two parts; one is translating camera's RGB value into tristimulus values, the other is estimating tristimulus values which users perceive from tristimulus values produced by former method. The latter multiplies attenuation values and each element of tristimulus values produced by the former method. They calculated attenuation values from spectral transmittance of an OST-HMD. There are few hue differences between the estimations and true background colors, but there are large Euclidean distances in the L*a*b* color space, corresponding to perceptual differences between them.

Studies by Zhang et al. [ZM18, ZMB21] are not about color compensation, but they conducted color matching experiments with an OST-HMD and estimated the reference color which users saw through an OST-HMD, using spectrum of the original reference color and OST-HMD's spectral transmittance. What these background color estimations have in common is that they focused on OST-HMD's spectral transmittance and treated it as a main factor of the background color shift.

We too focus on OST-HMD's spectral transmittance and think that the spectrum of the light through an OST-HMD can be estimated from the original spectrum and an OST-HMD's spectral transmittance. However, the above studies didn't report details of how they measured spectral transmittance, and they didn't account for the effect of viewing angle or position of the display. So we divided each OST-HMDs into nine smaller areas, measured the spectral transmittance of each area, and measured from different angles on the same area. By doing these, we investigated how viewing position and angle affect spectral transmittance. In addition, we report the details of the 3D printed measuring instruments and how we conducted measurements with these tools.

3. Methods of Measurement

3.1. Notation

Here, we describe the notations used in following sections. s_{dir} refers to the spectrum of the original background light and s_{hmd} means the spectrum of the background light which passes through an OST-HMD. s_{trans} refers to an OST-HMD's spectral transmittance. s_{calc} is the reproduction of s_{hmd} calculated by multiplying each wavelength component of s_{dir} and s_{trans}. Tristimulus values corresponding to s_{dir}, s_{hmd} and s_{calc} are denoted as c_{dir}, c_{hmd} and c_{calc}, respectively.

In this study, we divided the rendering area of each OST-HMD into nine grids, and measurements were taken for each area. If we divided the rendering area more finely, we could get a spatially more precise measurement. However, the smaller a measuring area becomes, the less light passes through. Thus, measuring accuracy drops. In addition, all measuring in this study was done manually, so dividing the count by more than nine was not feasible. The abbreviations of these areas are UR, U, UL, R, C, L, DR, D and DL, which stand for Up-Right, Up, Up-Left, Right, Center, Left, Down-Right, Down and Down-Left, respectively.

In addition, we also took measurements from three different angles for the area C. One was made on the same height of the center of the area C, the other two were taken from positions that were 4-5 millimeters higher and lower than the center. We refer to measurements made on the higher position as "High" and lower one as "Low."

Figure 2: *Color samples and sRGB values of the background*

3.2. Overview of Measurement Procedures

We used thirteen sheets of colored paper, size B4, as the background. These colors were chosen from twenty-nine colored papers available in the store nearby our university. We had excluded resembling colors and dark colors which can't reflect light in enough brightness to measure, then these thirteen colors remained. Samples of these colors and their sRGB values are shown in Figure 2 as a reference. These were translated from the measured tristimulus values under a light source that is detailed later. We used the Y of color #1's tristimulus values as a white point for this translation.

We made nine masks that have an aperture on the position corresponding to each measuring areas. And also, we measured from two additional measuring angles (High and Low) for the area C. Thus, there were $3 \times 13 \times 11 = 429$ measuring conditions (3 OST-HMDs, 13 background colors and 11 measuring areas and angles). The two spectra (s_{hmd} and s_{dir}) are measured three times and averaged for each condition, so $429 \times 2 \times 3 = 2574$ measurements were made in total. The measuring procedures were as follows:

1. Set the OST-HMD, colored paper, mask and spectrometer on the measurement instruments.
2. Cover the spectrometer with black felt to block light other than that passed through a mask's aperture.
3. Measure the spectrum of light from the background (s_{hmd}) three times to mitigate measuring error.
4. Remove the OST-HMD and measure spectrum (s_{dir}) three more times.
5. Replace the colored paper with another and repeat procedures 1-4. There are 13 background colors, so these procedures are repeated 13 times in total.
6. Once measurements are made for all background colors, replace the mask with an another and repeat procedures 1-5 again. There are 9 masks and additional measures High and Low for the area C, so procedures 1-5 are repeated 11 times in total.
7. Once measurements are made for all masks and angles, replace the OST-HMD with an another and repeat procedures 1-6. For the 3 OST-HMDs, procedures 1-6 are repeated 3 times in total.

3.3. OST-HMDs and Other Equipment

3.3.1. Target OST-HMDs

In this study, we chose the Magic Leap 1, the HoloLens (first gen) and the HoloLens 2 as targets of measure. Hereafter, we refer to them as ML, HL1 and HL2. The reason of choice is because they are off-the-shelf devices and they have been in research [ZWP*21, EMP*17, PHNG20] and commercial use.

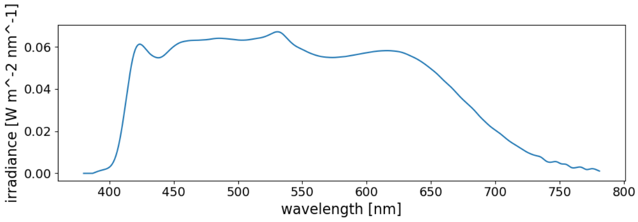

Figure 3: *Spectrum distribution of a common desklight, part number TG008-D0001TY.*

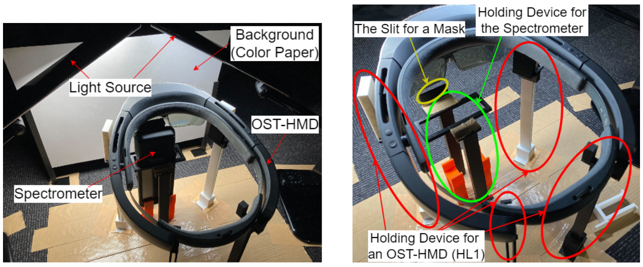

(a) *Actual setting used for measurements.* **(b)** *Fixtures for the Spectrometer and the HoloLens 1.*

Figure 4: *Images of the measurement environment and instruments used to gather data.*

3.3.2. Spectrometer and Light Source

We used the Sekonic C-7000 SPECTROMASTER. This spectrometer can measure the light spectrum from 380[nm] to 780[nm] in 1[nm] increments. We set the measuring range as "L", measuring mode to "Ambient Light" and exposure time to "Auto" for all measures.

We used a Toyoda Gosei LED light (part number TG008-D0001TY) as the light source because of its wide spectrum distribution. Figure 3 shows spectrum distribution of this light measured by the previously mentioned spectrometer. The brightness of this light can be adjusted, and we set the brightness to maximum for all measures. Its brightness is 4310[lx] and its color temperature is 5930[K].

3.4. Measuring Instruments

The measuring instruments consist of 3D printed fixtures designed to hold the displays and spectrometer as well as masks that constrict the measurement area.

3.4.1. Device Fixtures

In order to measure under certain conditions, the OST-HMDs and spectrometer were attached to fixtures (Figure 4a), which were specialized for each target HMD. The fixture for the HL1 uses four pillars for support (the red circles in Figure 4b). The fixture for the HL2 has a base-like table instead of rear pillars in a fixture for the HL1, because HL2 has the heavier buckle on the back and it can't be supported by pillars. The fixtures for the ML and HL1 support the HMD with pillars. However, there are cables on the back of the ML, thus three pillars on the nose bridge and side band are used.

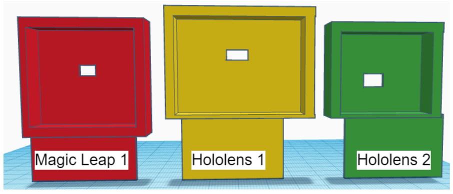

Figure 5: *CAD models of the masks fitted to each individual display.*

The fixture for the spectrometer (a green circle in Figure 4b) is independent of one for an OST-HMD. The spectrometer was set into the orange bases shown in Figure 4b, which allowed for variable height, and thus variable measuring angles. In order to measure High and Low, we raised or lowered these bases as much as the height of the mask's aperture, because the dimensions of mask's aperture differed among the target OST-HMDs, and we wanted to align a lens of the spectrometer and a mask's hole similarly among target OST-HMDs. In addition, the fixture for the spectrometer holds not only the spectrometer, but also the mask. Each mask is inserted into a slit in the device (the yellow circle in Figure 4b), and the positioning of the spectrometer and mask are fixed.

And also the background colored paper is fixed in front of an OST-HMD. There are two fixed pillars with a slit, and a colored paper is inserted into both slits and fixed.

3.4.2. Masks

Figure 5 shows CAD models of masks which block light from outside of the measuring area. They have an aperture which corresponding to one of the measuring area and have a cover on peripheral which blocks unnecessary external light. We used masks which have different dimensions according to target OST-HMDs. Dimensions of an aperture also differ according to target OST-HMDs, because dimensions of displays differ and so do dimensions of each measuring areas. Left red mask in Figure 5 is used for ML, center yellow one is used for HL1, right green one is used for HL2. We printed nine masks which have an aperture on different position for each OST-HMDs.

3.5. Measuring Environment

Measurements were made in a dark room. A piece of colored paper was put about 10 cm from the front of each OST-HMD. We used different fixtures for each target OST-HMDbut used the same environment for all OST-HMDs. In actual measure, a piece of black felt covered each OST-HMD and the spectrometer in order to block unnecessary light from above or the side.

4. Evaluation Method

We measured s_{dir} and c_{dir} by measuring the light from background directly and measured s_{hmd} and c_{hmd} by measuring the light which passes through an OST-HMD. We compared them and studied how the background color is shifted by an OST-HMD.

4.1. Calculation of Spectral Transmittance

The s_{trans} of an area of an OST-HMD is calculated with s_{dir} and s_{hmd} measured on the same area. Spectral irradiance of s_{dir} and s_{hmd} in λ [nm]is described as $s^{\lambda}_{\text{hmd}}, s^{\lambda}_{\text{dir}}$ $[\text{W} \cdot \text{m}^{-2} \cdot \text{nm}^{-1}]$. Transmittance of s_{trans} in λ [nm], $s^{\lambda}_{\text{trans}}$ $[\cdot]$is calculated by the equation 1.

$$s^{\lambda}_{\text{trans}} = \frac{s^{\lambda}_{\text{hmd}}}{s^{\lambda}_{\text{dir}}} \tag{1}$$

$s^{\lambda}_{\text{trans}}$ is calculated in 1[nm] increments. In order to mitigate measuring errors, we measured s_{dir} and s_{hmd} three times each and took averages of them by calculating averages in 1[nm] increments.

Although the spectrometer we used in this study can measure spectrum from 380 [nm] to 780 [nm], spectral irradiance of the light source around 400 [nm] or 700 [nm] is relatively small as Figure 3 shows and there are less confidence in measurements around these bandwidth. Thus, we don't use measurements in all bandwidth but only in a reliable bandwidth. Reliable bandwidth is determined by the following method. For every measuring conditions, spectral irradiance of 3 measurements at λ [nm] is denoted as $l^{\lambda}_1, l^{\lambda}_2, l^{\lambda}_3$ $[\text{W} \cdot \text{m}^{-2} \cdot \text{nm}^{-1}]$. Then the difference between largest and smallest among them e^{λ}, the average of them l^{λ} and the ratio of e^{λ} to l^{λ}, r^{λ} can be calculated.

$$e^{\lambda} = \max\{l^{\lambda}_1, l^{\lambda}_2, l^{\lambda}_3\} - \min\{l^{\lambda}_1, l^{\lambda}_2, l^{\lambda}_3\} \tag{2}$$

$$l^{\lambda} = \frac{\sum_{i=1}^{3} l^{\lambda}_i}{3}, \qquad r^{\lambda} = \frac{e^{\lambda}}{l^{\lambda}} \tag{3-4}$$

The illuminance accuracy of the spectrometer is $\pm 5\%$ according to the specification sheet. The spectral irradiance accuracy is not on the specification sheet, however illuminance can be calculated from spectral irradiance, so we decided to consider the accuracy of spectral irradiance $\pm 5\%$ as well as illuminance irradiance. If there are 5% up or down in $l^{\lambda}_1, l^{\lambda}_2, l^{\lambda}_3$ from the average l^{λ}, r^{λ} is 10%. If $r^{\lambda} > 10\%$, there are greater gap than 5% between l^{λ} and at least one measurements $(l^{\lambda}_1, l^{\lambda}_2, l^{\lambda}_3)$, thus l^{λ} isn't reliable as a true value. Therefore we considered a reliable bandwidth as a consecutive bandwidth which r^{λ} is lesser than 10% in all measuring conditions. We analyzed the measurement results and got a bandwidth from 421 [nm] to 709 [nm] as a reliable bandwidth.

4.2. Calculation of Tristimulus values

In this study, tristimulus values are used to evaluate the color of light that users perceive when they see it. The spectrometer we use can measure tristimulus values, but its calculation method is not public, and we want to calculate tristimulus values for not only the measured spectrum but also for the calculated spectrum s_{calc}. Thus we declared the calculation method and used it to get tristimulus values for all spectra, including the one we measured.

We denote the spectrum of spectral irradiance as s_{abs} and its value at λ [nm] as s^{λ}_{abs} $[\text{W} \cdot \text{m}^{-2} \cdot \text{nm}^{-1}]$. We can calculate the relative spectrum s_{rel} by normalizing s_{abs} to make the maximum value 1.

$$s^{\lambda}_{\text{rel}} = \frac{s^{\lambda}_{\text{abs}}}{s^{\max}_{\text{abs}}} \tag{5}$$

s^{λ}_{rel} $[\cdot]$ is a value of s_{rel} at λ [nm] and $s^{\max}_{\text{abs}}$ $[\text{W} \cdot \text{m}^{-2} \cdot \text{nm}^{-1}]$ is the maximum spectral irradiance of s_{abs} between reliable bandwidth. Then, we can calculate tristimulus values using s_{rel} and color-matching functions of the CIE 1964 standard colorimetric system.

Tristimulus values X, Y, Z can be calculated by equation 4.2.

$$X = \sum_{\lambda} s^{\lambda}_{\text{rel}} x^{\lambda},\ Y = \sum_{\lambda} s^{\lambda}_{\text{rel}} x^{\lambda},\ Z = \sum_{\lambda} s^{\lambda}_{\text{rel}} z^{\lambda} \tag{6}$$

$x^{\lambda}, y^{\lambda}, z^{\lambda}$ are values of color-matching functions at λ [nm]. The range of λ is a reliable bandwidth, from 421 [nm] to 709 [nm].

4.3. Translation from Tristimulus values to L*a*b* Color Space

L*a*b* color space is a color space where a perceptual difference between two colors is proportional to a distance between them in that color space. We translate tristimulus values into the coordinates in L*a*b* color space in order to evaluate a perceptual difference among them. The values of a coordinate in L*a*b* color space L^*, a^*, b^* can be calculated from tristimulus values by equations specified by CIE (Commission Internationale de l'Eclairage) [ISO19]. This calculation requires an arbitrary white point. We used tristimulus values of the illuminant D65 spectrum calculated by a method described in section 4.2 as a white point. The specific values of a white point (X_n, Y_n, Z_n) are as follows.

$$X_n = 91.88,\ Y_n = 98.45,\ Z_n = 98.40 \tag{7}$$

4.4. Color Comparison in L*a*b* Color Space

L*a*b* color space was designed to express just noticeable difference as 1 euclidean distance in that space. However, L*a*b* color space is not completely uniform, thus there are some problems, e.g. euclidean distances of just noticeable difference among saturated colors and around neutral colors are different. In order to overcome these shortcomings, a metric CIEDE 2000 was developed [LCR01]. It is not just euclidean distance in the color space, but has some corrections to address nonuniformity of L*a*b* color space. Therefore we used CIEDE 2000 (denoted as ΔE_{00}) as a metric which expresses a perceptual difference between two coordinates in L*a*b* color space and regarded $\Delta E_{00} = 1$ as the just noticeable difference. A bigger ΔE_{00} means a bigger perceptual difference, and if the ΔE_{00} between two colors is bigger than 1, there is a sufficiently perceptible difference between them.

4.5. Evaluation Indices

ΔE^{dh}_{00} means CIEDE 2000 between L*a*b* coordinates of c_{dir} and c_{hmd}. If $\Delta E^{dh}_{00} > 1$, it can be said that a target OST-HMD shifts the background color so much that users perceive.

ΔE^{hc}_{00} means CIEDE 2000 between L*a*b* coordinates of c_{hmd} and c_{calc}. If $\Delta E^{hc}_{00} < 1$, it can be said that c_{calc} is close enough to c_{hmd} and measuring accuracy of spectral transmittance used to calculate c_{calc} is enough.

In order to examine spectral transmittance uniformity of each OST-HMDs, we compared c_{calc} and c'_{calc}, which is tristimulus values calculated from spectral transmittance of the area C in target OST-HMD and the same s_{dir} used to calculate c_{calc}. CIEDE 2000 between

Table 1: *Averages of ΔE_{00}^{dh} and $\Delta E_{00}^{cc'}$ for each OST-HMDs.*

OST-HMD	ΔE_{00}^{dh} avg.	$\Delta E_{00}^{cc'}$ (High) avg.	$\Delta E_{00}^{cc'}$ (Low) avg.
ML	6.08	2.70	1.58
HL1	9.31	0.96	0.79
HL2	6.18	1.94	1.39

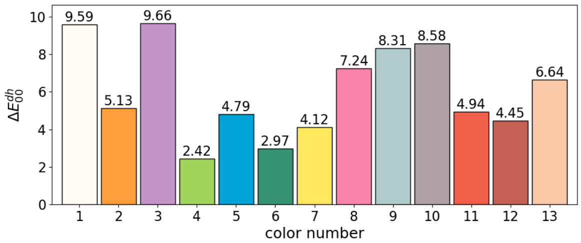

Figure 6: ΔE_{00}^{dh} *averages for each background colors (ML).*

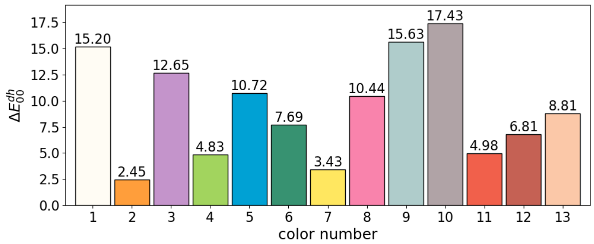

Figure 7: ΔE_{00}^{dh} *averages for each background colors (HL1).*

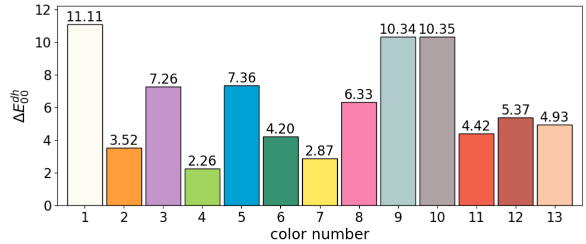

Figure 8: ΔE_{00}^{dh} *averages for each background colors (HL2).*

them is $\Delta E_{00}^{cc'}$. If $\Delta E_{00}^{cc'} < 1$, it can be said that c_{calc} and c'_{calc} are close enough and spectral transmittance used to calculate c_{calc} and one of the area C used to calculate c'_{calc} are close enough too. It means that spectral transmittance of the OST-HMD is uniform enough. Under our measuring condition, the background was not lit uniformly. Thus, lights from two different areas could not be compared, so we compared c_{calc} and c'_{calc} instead of comparing c_{hmd} of each area.

In order to examine how the measuring angle affects spectral transmittance, we used $\Delta E_{00}^{cc'}$ of High and Low. Here, c'_{calc} is tristimulus values calculated from s_{dir} of High or Low and spectral transmittance measured from normal height.

5. Results

In this section, we report results of measures. However there are too many data to report all of them here, thus we report only analysis results of measurements.

5.1. Magnitude of Background Color Shifts

We analysed ΔE_{00}^{dh} and examined how background colors are shifted by OST-HMDs. Table 1 shows averages of ΔE_{00}^{dh} calculated using all measurements of each OST-HMDs. It indicated that the HL1 shifts background colors the most, next is the HL2 and the ML shifts the least. However, all of averages in Table 1 are six times or greater than 1, i.e., the threshold of perceptible difference, so we can conclude that all of the OST-HMDs shift the background colors significantly and perceptibly.

Figures 6, 7, and 8 show the averages of ΔE_{00}^{dh} for each of the background colors. There are differences in ΔE_{00}^{dh} among background colors for all OST-HMDs, thus certain background colors are shift more significantly than others. This is extremely important to take into account when designing color compensation hardware or algorithms. These also have similar trends, e.g. neutral colors (1, 9, 10) and bluish colors (3, 5, 8) have a relatively larger ΔE_{00}^{dh}.

5.2. Uniformity of Spectral Transmittance

Table 2 shows averages of $\Delta E_{00}^{cc'}$ for each areas of OST-HMDs. $\Delta E_{00}^{cc'}$ is not calculated for area C, because $\Delta E_{00}^{cc'}$ is a metric which expresses difference of spectral transmittance between area C and targeting area. Large $\Delta E_{00}^{cc'}$ ($\Delta E_{00}^{cc'} > 1$) means that there is a so much difference between spectral transmittance of area C and targeting area that there is a difference users can perceive between colors of light through these areas from same background. Table 2 indicates that HL1 has more uniform spectral transmittance than ML or HL2. On the other hand, HL2 seems to have least uniform spectral transmittance. $\Delta E_{00}^{cc'}$ of every areas in HL2 is greater than 1. However, even HL1 has large $\Delta E_{00}^{cc'}$ on bottom areas (DL, D, DR), thus none of them has completely uniform spectral transmittance.

Figure 9a, 9b, 9c show average spectral transmittance of each areas. These seem that spectral transmittance of HL1 have more variance than ML and it may seem to be incompatible with the results of Table 2. However, distances among plots of spectral transmittance are not as important as differences in their shape. Because the spectrum of light is normalized when tristimulus values is calculated, thus two spectral transmittance which have same shape in different magnitudes produce the same tristimulus values. Therefore, it can be said that the uniformity of spectral transmittance is the uniformity of the shape of the spectral transmittance when the uniformity of background color matters.

In order to examine the uniformity of the shape of spectral transmittance in Figures 9a, 9b, and 9c, we divide the values of each spectral transmittance by values of spectral transmittance of area C in 1 [nm] incriments and plot them. Spectral transmittance of area C will be a horizontal line at $y = 1$ and spectral transmittance which will resemble area C, will be close to a horizontal line. Comparing Figure 10a, 10b shows that plots in Figure 10b are more close to horizontal lines and Figure 10b has less crossing among plots than Figure 10a. Plots in Figure 10c are the farthest from horizontal lines and there are the most crossing among plots, showing that the HL1 has the most uniform spectral transmittance and HL2 has the worst.

Table 2: *Averages of the perceptual differences $\Delta E_{00}^{cc'}$ between different displays and screen areas.*

OST-HMD	Area	Average of $\Delta E_{00}^{cc'}$	Area	Average of $\Delta E_{00}^{cc'}$	Area	Average of $\Delta E_{00}^{cc'}$
Magic Leap	Up-Left	2.08	Up	2.28	Up-Right	1.65
	Left	1.89	Center	-	Right	0.34
	Down-Left	1.66	Down	0.85	Down-Right	1.32
HoloLens 1	Up-Left	0.87	Up	0.90	Up-Right	0.60
	Left	0.54	Center	-	Right	0.76
	Down-Left	2.10	Down	1.61	Down-Right	2.23
HoloLens 2	Up-Left	2.67	Up	2.80	Up-Right	3.47
	Left	2.91	Center	-	Right	2.56
	Down-Left	2.96	Down	3.03	Down-Right	1.89

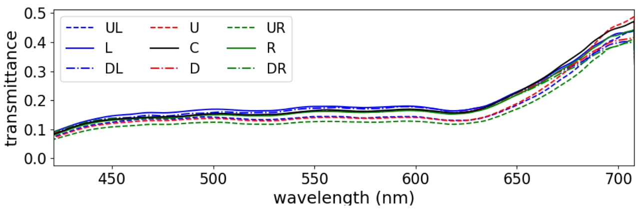

(a) *Magic Leap*

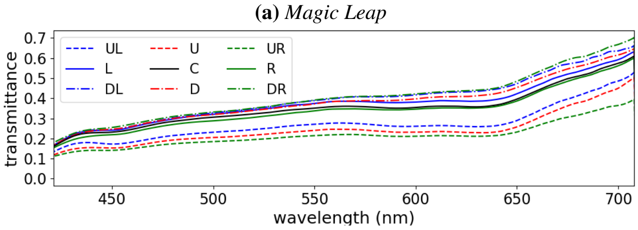

(b) *HoloLens 1*

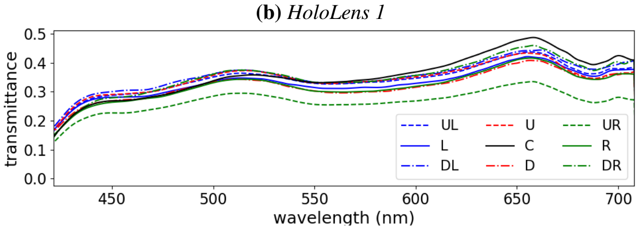

(c) *HoloLens 2*

Figure 9: *Spectral transmittance of each area.*

However, difference in absolute values among spectral transmittance leads difference in brightness. Thus, even if there are little difference in background colors among areas when they are individually measured by spectrometers, difference in brightness may lead that users perceive difference when they see all areas at the same time. In addition, if there are large difference in brightness of background, it becomes harder to display each contents in same brightness. Therefore, the better the color uniformity of a given OST-HMD, the easier it should be to carry out color compensation.

Table 1 shows averages of $\Delta E_{00}^{cc'}$ at area C measured from High and Low positions. These results indicate that measuring angle affects spectral transmittance of ML and HL2 so much that users can perceive, but spectral transmittance of HL1 is less affected.

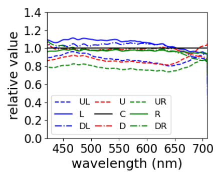

(a) *Magic Leap*

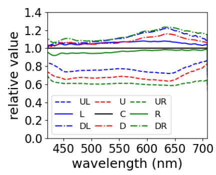

(b) *HoloLens 1*

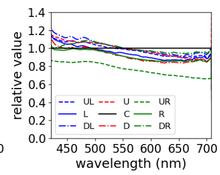

(c) *Hololens 2*

Figure 10: *Spectral transmittance of each area, transformed with respect to area C.*

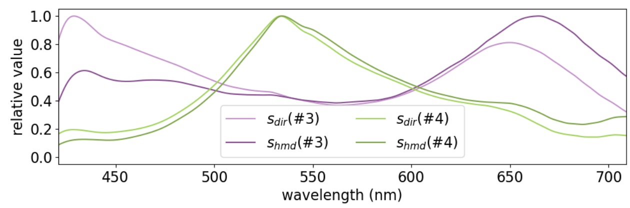

Figure 11: s_{dir} *and* s_{hmd} *of color 3 and 4.*

6. Discussion

6.1. Effect of Background Color Shift

As Table 1 shows, we found that for all OST-HMDs, an OST-HMD shifts background colors. Thus, it can be hard to do precise color compensation by simply using an image from an external camera that sees the background. In section 5.1, we found that certain colors shift more than others. For example, neutral colors tend to have larger ΔE_{00}^{dh}. The reason of this can be guessed that neutral colors have a uniform spectrum that spreads over a wide range of wavelengths, and spectral transmittance disrupts that balance. Thus, the shape of spectrum is changed greatly.

Bluish colors also tend to have a larger ΔE_{00}^{dh}. The reason for this may be that the peak of the bluish color spectrum is in a shorter wavelength band, and the spectral transmittance of each OST-HMD has less transmittance around short wavelengths than long ones. Thus, the peak is shifted and the shape of the spectrum is changed significantly. Figure 11 shows an example of this. This figure shows normalized s_{dir} and s_{hmd} of color number 3 and 4 through HL1. Background color 3 is purple and 4 is green (Figure 2). By comparing the spectrum in Figure 11, we find that the peak of No.3's spectrum, which was originally around 400 [nm], shifted to around 650 [nm] and the shape of the spectrum changed more than No.4.

Difference in amount of background color shift may affect usability in some aspects. Contrast between output of an OST-HMD and background may be one of them. For example, Kruijff et al. [KOK*18] conducted user experiments which examined visibility of UIs displayed on an OST-HMD and VST-HMD, and they found that users most preferred blue, and the percentage of OST-HMD users who preferred blue was 10 points more than a VST-HMD user. They suggested that this is because blue has the biggest contrast with the background. If their OST-HMD had similar spectral transmittance to ones in this study, spectral transmittance might contribute to enhance contrast between blue contents and background by diminishing blue elements in background colors. Like this, we may be able to find content colors which can maintain a high contrast with background by examining spectral transmittance and color shifts.

6.2. Effect of Areas and Angles on Background Color Shift

The three OST-HMDs we used did not have completely uniform spectral transmittance. In practice, this result indicates that the unevenness of spectral transmittance should be taken into account, like in the compensation method proposed by Langlotz et al. [LCR16]. Pixelwise color compensation requires background color which users see through each pixels. If how background color shifts depends on only its position in display, it can be calculated in advance for each pixel. Thus, it may not be so hard to calculate background colors which users see with images from external cameras. On the other hand, if the shift depends on viewing angle, additional real time calculation based on information about user's eyes and display positioning is required. Therefore, consistency of spectral transmittance across viewing angle is more important than uniformity across the display. By looking at Table 2, it can be said that HL1 has the best consistency and it's cut out for color compensation the best in OST-HMDs used in this study.

6.3. Measuring Accuracy of Spectral Transmittance

By examining ΔE_{00}^{hc}, we evaluated our measuring accuracy of spectral transmittance. If $\Delta E_{00}^{hc} < 1$, the calculated background color through an OST-HMD (c_{calc}) is close enough to real background color through an OST-HMD (c_{hmd}), thus it can be said that spectral transmittance used to calculate c_{calc} was measured in sufficient accuracy. We calculated ΔE_{00}^{hc} for all combinations of OST-HMDs, background colors (except color number 1, which is used to calculate spectral transmittance), areas and measuring angles and found that the percentage of data with ΔE_{00}^{hc} lower than 1 was about 57.3%.

This accuracy may not be adequate for complete color compensation, so there is some room for improvement here. We analyzed data and found that there are areas which have many $\Delta E_{00}^{hc} > 1$ data and areas which have less $\Delta E_{00}^{hc} > 1$ data. We used the same instruments to measure different areas, except masks, which had the same dimensions except for aperture position. Thus, it's hard to say that instruments are cause of accuracy drop. One possible cause is insufficient brightness of background. Tristimulus values are calculated using normalized spectrum and if max value of spectrum is small, slight measuring error will be large error in normalized

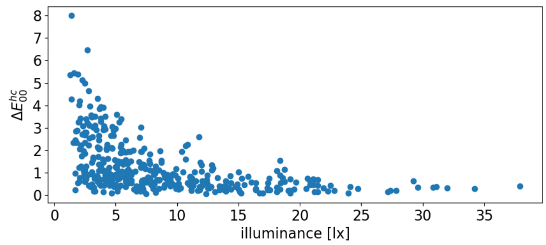

Figure 12: *The relationship between ΔE_{00}^{hc} and background illuminance.*

spectrum. Our light source did not light the background uniformly, thus different areas had different background brightness, and this could cause a bias of ΔE_{00}^{hc} between areas.

We plotted all data (except color number 1) in Figure 12. It shows that data which has big ΔE_{00}^{hc} is concentrated in small illuminance area. We also performed correlation analysis and got correlation coefficient about -0.49. We calculated the percentage of $\Delta E_{00}^{hc} < 1$ data using data whose illuminance is greater that 10 [lx] only, then we got about 86.3%. This indicates that our procedure can measure spectral transmittancein sufficient accuracy if illuminance is enough. Therefore, enlargement of background illuminance by replacing light source into more stronger one or replacing background colored papers into other material which has higher reflectance may improve the measuring accuracy of spectral transmittance.

7. Conclusion

In this study, we objectively measured the characteristics of background color shifts seen through three different OST-HMDs using the CIEDE 2000. We also analyzed these characteristics in detail in order to contribute to future studies and methods for optical see-through color compensation. We first confirmed the extent to which OST-HMDs shift background color, finding that all three of the OST-HMDs we used (ML, HL1 and HL2) shift background color in a manner perceptible by the end-user. We also found that some background colors shift more than others and provided a detailed analysis of these shifts, which is important both for the design of future HMD optics. Blue components were more diminished, which means that contrast between content and background is likely to increase in this band.

We focused on spectral transmittance as the main factor of background color shifts and examined uniformity and consistency of the spectral transmittance across measuring angles. We found that the HoloLens 1 has a more uniform spectral transmittance except for its bottom areas. On the other hand, the spectral transmittance of the HoloLens 2 and Magic Leap is less uniform, and background colors shift differently in different areas of these OST-HMDs. The HoloLens 1 also had the best spectral consistency. For the other two OST-HMDs, the background color shifts depend on viewing angle. These results indicate that compensation techniques not only need to take background into account, but must also consider position of content in the display and position relative to the user's eye for precise color compensation.

References

[AGBAD*21] AVILA-GARZON C., BACCA-ACOSTA J., DUARTE J., BETANCOURT J., ET AL.: Augmented Reality in Education: An Overview of Twenty-Five Years of Research. *Contemporary Educational Technology 13*, 3 (2021). 1

[DPMS18] DE PACE F., MANURI F., SANNA A.: Augmented reality in industry 4.0. *American Journal of Computer Science and Information Technology 6*, 1 (2018), 17. 1

[EHRSMR19] ESCALADA-HERNÁNDEZ P., RUIZ N. S., SAN MARTÍN-RODRÍGUEZ L.: Design and evaluation of a prototype of augmented reality applied to medical devices. *International journal of medical informatics 128* (2019), 87–92. 1

[EMP*17] EVANS G., MILLER J., PENA M. I., MACALLISTER A., WINER E.: Evaluating the Microsoft HoloLens through an augmented reality assembly application. In *Degraded environments: sensing, processing, and display 2017* (2017), vol. 10197, International Society for Optics and Photonics, p. 101970V. 3

[GSZ13] GABBARD J. L., SWAN J. E., ZARGER A.: Color blending in outdoor optical see-through AR: The effect of real-world backgrounds on user interface color. In *2013 IEEE Virtual Reality (VR)* (2013), pp. 157–158. 1, 2

[GSZW10] GABBARD J. L., SWAN J. E., ZEDLITZ J., WINCHESTER W. W.: More than meets the eye: An engineering study to empirically examine the blending of real and virtual color spaces. In *2010 IEEE Virtual Reality Conference (VR)* (2010), IEEE, pp. 79–86. 1, 2

[HGH*01] HAVIG P. R., GRIGSBY S. S., HEFT E. L., LACRETA J. M., POST D. L.: Luminance contrast and color recognition in helmet-mounted displays. In *Helmet-and Head-Mounted Displays VI* (2001), vol. 4361, International Society for Optics and Photonics, pp. 198–204. 2

[HRISI15] HINCAPIÉ-RAMOS J. D., IVANCHUK L., SRIDHARAN S. K., IRANI P. P.: SmartColor: real-time color and contrast correction for optical see-through head-mounted displays. *IEEE Transactions on Visualization and Computer Graphics 21*, 12 (2015), 1336–1348. 1, 2

[ILI*19] ITOH Y., LANGLOTZ T., IWAI D., KIYOKAWA K., AMANO T.: Light attenuation display: Subtractive see-through near-eye display via spatial color filtering. *IEEE transactions on visualization and computer graphics 25*, 5 (2019), 1951–1960. 2

[ILSP21] ITOH Y., LANGLOTZ T., SUTTON J., PLOPSKI A.: Towards indistinguishable augmented reality: A survey on optical see-through head-mounted displays. *ACM Computing Surveys (CSUR) 54*, 6 (2021), 1–36. 2

[ISO19] ISO/CIE 11664-4 (2019): Colorimetry—Part 4: CIE 1976 L* a* b* colour space. 5

[KOK*18] KRUIJFF E., ORLOSKY J., KISHISHITA N., TREPKOWSKI C., KIYOKAWA K.: The influence of label design on search performance and noticeability in wide field of view augmented reality displays. *IEEE transactions on visualization and computer graphics 25*, 9 (2018), 2821–2837. 8

[LBS] LIVINGSTON M. A., BARROW J. H., SIBLEY C. M.: Quantification of contrast sensitivity and color perception using head-worn augmented reality displays. In *2009 IEEE Virtual Reality Conference*, pp. 115–122. 2

[LCR01] LUO M. R., CUI G., RIGG B.: The development of the CIE 2000 colour-difference formula: CIEDE2000. *Color Research & Application: Endorsed by Inter-Society Color Council, The Colour Group (Great Britain), Canadian Society for Color, Color Science Association of Japan, Dutch Society for the Study of Color, The Swedish Colour Centre Foundation, Colour Society of Australia, Centre Français de la Couleur 26*, 5 (2001), 340–350. 1, 5

[LCR16] LANGLOTZ T., COOK M., REGENBRECHT H.: Real-time radiometric compensation for optical see-through head-mounted displays. *IEEE transactions on visualization and computer graphics 22*, 11 (2016), 2385–2394. 1, 2, 8

[Lee12] LEE K.: Augmented reality in education and training. *TechTrends 56*, 2 (2012), 13–21. 1

[MF13] MAIMONE A., FUCHS H.: Computational augmented reality eyeglasses. In *2013 IEEE International Symposium on Mixed and Augmented Reality (ISMAR)* (2013), IEEE, pp. 29–38. 2

[PHNG20] PARK B. J., HUNT S. J., NADOLSKI G. J., GADE T. P.: Augmented reality improves procedural efficiency and reduces radiation dose for CT-guided lesion targeting: a phantom study using HoloLens 2. *Scientific Reports 10*, 1 (2020), 1–8. 3

[PYK19] PARK Y., YUN S., KIM K.-H.: When IoT met augmented reality: Visualizing the source of the wireless signal in AR view. In *Proceedings of the 17th Annual International Conference on Mobile Systems, Applications, and Services* (2019), pp. 117–129. 1

[RKLK16] RYU J.-H., KIM J.-W., LEE K.-K., KIM J.-O.: Colorimetric background estimation for color blending reduction of OST-HMD. In *2016 Asia-Pacific Signal and Information Processing Association Annual Summit and Conference (APSIPA)* (2016), IEEE, pp. 1–4. 2

[SHRFI13] SRIDHARAN S. K., HINCAPIÉ-RAMOS J. D., FLATLA D. R., IRANI P.: Color correction for optical see-through displays using display color profiles. In *Proceedings of the 19th ACM Symposium on Virtual Reality Software and Technology* (2013), pp. 231–240. 1, 2

[WHL10] WETZSTEIN G., HEIDRICH W., LUEBKE D.: Optical image processing using light modulation displays. In *Computer Graphics Forum* (2010), vol. 29, Wiley Online Library, pp. 1934–1944. 2

[YLD*21] YEO S. M., LIM J. Y., DO J. G., LIM J.-Y., LEE J. I., HWANG J. H.: Effectiveness of interactive augmented reality-based telerehabilitation in patients with adhesive capsulitis: protocol for a multi-center randomized controlled trial. *BMC musculoskeletal disorders 22*, 1 (2021), 1–9. 1

[ZM18] ZHANG L., MURDOCH M. J.: Color matching criteria in augmented reality. In *Color and Imaging Conference* (2018), vol. 2018, Society for Imaging Science and Technology, pp. 102–109. 3

[ZMB21] ZHANG L., MURDOCH M. J., BACHY R.: Color appearance shift in augmented reality metameric matching. *JOSA A 38*, 5 (2021), 701–710. 3

[ZWP*21] ZHANG Y., WANG R., PENG E. Y., HUA W., BAO H.: Color Contrast Enhanced Rendering for Optical See-through Head-mounted Displays. *IEEE Transactions on Visualization and Computer Graphics* (2021). 1, 2, 3